Agromet 37 (1): 34-43, 2023

Agromet
journal.ipb.ac.id/index.php/agromet
ISSN : 0126 - 3633

The Study of Wind Field ERA-20C in Monsoon Domains for Rainfall Predictor in Indonesia (Java, Sumatra, and Borneo)

Trinah Wati[1,2], Tri Wahyu Hadi[1], Ardhasena Sopaheluwakan[2], Lambok M. Hutasoit[1]

[1]Graduate Program of Earth Sciences, Faculty of Earth Sciences and Technology, Institut Teknologi Bandung, Bandung, Indonesia 40132

[2]Indonesia Agency for Meteorology, Climatology, and Geophysics, Jakarta, Indonesia 10610

ARTICLE INFO

Received
15 January 2023

Revised
09 March 2023

Accepted for Publication
05 May 2023

Published
31 May 2023

doi: 10.29244/j.agromet.37.1.34-43

Correspondence:
Trinah Wati
Indonesia Agency for Meteorology, Climatology, and Geophysics, Jakarta, Indonesia 10610
Email: trinah.wati@bmkg.go.id

ABSTRACT

In recent years, various research institutions have developed diverse global data reanalysis projects. This provides an opportunity to gain long-term of meteorological data for local scale. This study aims to select the potential predictor of wind fields u and v of the ERA-20C dataset, a reanalysis dataset, at 850 mb from seven domains or windows of Asian, Maritime Continent, Australian, and Western North Pacific monsoon related physically to rainfall anomaly patterns in Indonesia. The vector wind velocity scalar was obtained by using a Helmholtz decomposition to separate the total circulation v = (u,v) into the divergent component/velocity potential (χ) or Phi and rotational component/stream function (ψ) or Psi for obtaining the scalar variable of vector wind velocity. The method applied Singular value decomposition (SVD) to identify pairs of spatial patterns (expansion coefficients) between the predictors of Phi and Psi in seven domains, with rainfall data from 48 stations in Java, Sumatra, and Borneo Islands from 1981 to 2010. The results revealed that spatial patterns correlations of Java Islands were the highest in the Maritime Continent monsoon domain (80°–150° E and 15°S–15° N), while Sumatra and Borneo Island were in the Western North Pacific monsoon domain (100°–130° E and 5°–15° N) with predictor Psi. The lowest correlation for Java, Sumatra, and Borneo was the Australian monsoon domain (110° E–130° E and 5° S–15° S) with predictor Phi. In general, spatial pattern correlations of Java Island were higher than others, agreeing with monsoonal rainfall type dominantly in the region.

KEYWORDS
potential predictor, reanalysis, singular value decomposition, spatial pattern, wind velocity

INTRODUCTION

The global atmospheric reanalysis system involves a prediction model, input observations, and assimilation to combine input observations with predictions for the short term. These systems provide the most accurate global estimation and analysis of past atmospheric conditions (SPARC, 2022). Recently, national meteorology services and universities, as well as national or international research institutes, have created different types of global data reanalysis. One of these reanalyses is ERA-20C, an ECMWF global reanalysis (Poli et al., 2016) that covered the period of the twentieth century (1900-2010). To improve the model's ability to simulate climate observations in the 20th century, ERA-20C uses surface pressure and wind observations for assimilation and 10 model ensembles from ERA-20CM data (Hersbach et al., 2015). It has a horizontal resolution of about 125 km (spectral truncation T159).

The availability of long-term global reanalysis da-

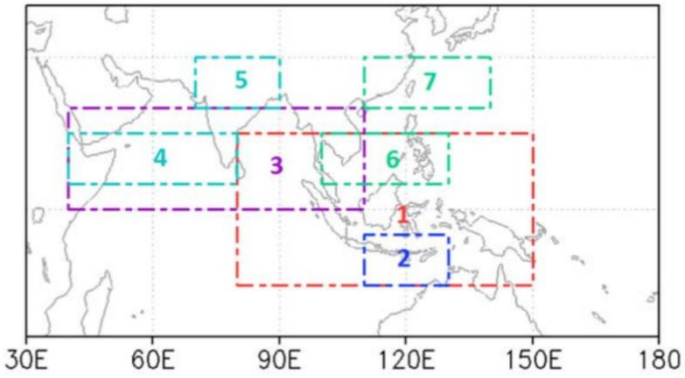

Figure 1. Seven-window domains of Maritime Continent: (1) Maritime Continent Monsoon (MCM) (80°−150° E and 15°S−15° N), (2) Australian Monsoon Index (AUSMI) (110°–130° E and 5°–15° S), (3) Webster and Young Monsoon Index (WYMI) (40°–110° E and 0°–20° N), (4) Indian Summer Monsoon (ISM) (40°–80° E and 5°–15° N), (5) Indian Summer Monsoon (ISM) (70°–90° E and 20°–30° N), (6) Western North Pacific Summer Monsoon (WNPSM) (100°–130° E and 5°–15° N), and (7) Western North Pacific Summer Monsoon (WNPSM) (110°–140° E and 20°–30° N).

-ta gives a prospect of reconstructing long-term local scale of meteorological data by conducting downscaling techniques (Donat et al., 2013; Jin et al., 2023). Caillouet, (2019) describe statistical down-scaling as extracting daily local-scale meteorological data from synoptic-scale atmospheric variables. The accuracy in selecting predictor variables in synoptic-scale determines the reliability of prediction or reconstuction statistical downscalling models (Mason and Baddour, 2008), and the selection of predictor domains or grid boxes (Back et al., 2013).

Indonesia's archipelago has high amounts of rainfall, which vary in spatial and temporal distribution throughout the year. This location is situated in the maritime continent, acting as a significant atmospheric heat source and contributing to the Hadley and Walker circulation on a planetary scale (Ramage, 1968). Indonesia's rainfall was strongly influenced by Asia-Australian monsoons, subdivided into monsoonal, semi-monsoonal, and anti-monsoonal types (Aldrian and Susanto, 2003; Hashiguchi et al. 2011; Lee, 2015). However, the monsoon patterns in Indonesia are complex due to various factors, such as the islands' topography and interactions with eastward-propagating and intra-seasonal oscillations, which cause significant differences in local-scale rainfall within a range of 50-100 km (Moron et al., 2010). Additionally, the inter-annual climate variability in Indonesia is influenced by the El Niño-Southern Oscillation (ENSO) (Hendon, 2003; Hendrawana et al., 2019; Hidayat and Andro, 2014).

This study aims to select the potential predictors of wind fields u and v at 850 mb from seven domains or windows of Asian and Australian Monsoons, which were related physically to rainfall anomaly patterns in Indonesia. The previous study (Surmaini et al., 2015; Syahputra, 2012) used those windows for the multi-windows approach in rainfall ensemble prediction for Sumatra and Java Regions but did not conduct a selection for the best window as the predictor. The seven windows were Maritime Continent Monsoon (MCM) (Robertson et al., 2011), Australian Monsoon Index (AUSMI) (Kajikawa et al., 2010), Webster and Young Monsoon Index (WYMI) (Webster and Yang, 1992), Indian Summer Monsoon (ISM) and Western North Pacific Summer Monsoon (WNPSM) (Wang et al., 2001) (Figure 1). This study pre-processed the ERA-20C dataset statistical downscaling analysis to select the appropriate window domains for rainfall ensemble prediction in Java, Sumatra and Borneo Islands of Indonesia.

RESEARCH METHODS

Data Source

The study employed 3-hourly zonal (u) and meridional (v) wind of the ERA-20C dataset at 850 mb from 1981-2010. The 3-hourly data were averaged with daily and monthly data. The stream function (ψ) or Psi and velocity potential (χ) or Phi to obtain the scalar variable of vector wind velocity. Phi and Psi were considered more appropriate for representing flow patterns in low latitudes, where geostrophic balance breaks down due to the small Coriolis parameter (Cao et al., 2022; Li et al., 2006; Palmer, 1952).

Previous studies (Surmaini et al., 2015; Syahputra, 2012) had used these predictors for predicting rainfall patterns in Indonesia. This research employed data obtained from 48 meteorological stations of BMKG (Indonesia Agency for Meteorology, Climatology and Geophysics) located in Java, Sumatra, and Borneo.

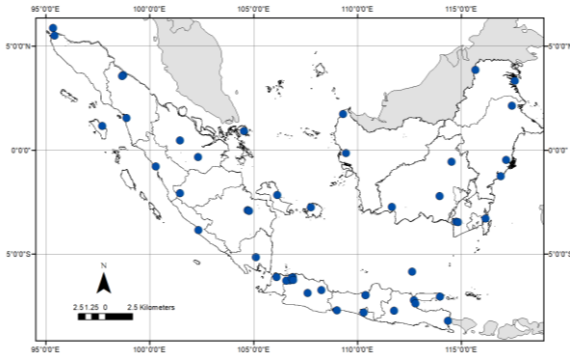

Figure 2. Distribution of rain gauge stations for rainfall verification in Java, Sumatra and Borneo used in the study.

Calculation Psi and Phi

The calculation of Psi and Phi used a decomposition of Helmholtz, which uniquely splits the total circulation $\vec{v}$ = (u, v) into divergent (vorticity free) or χ (Phi) and rotational (divergence free) components or ψ (Psi) (Dutton, 1976; Hammond and Lewis, 2021). The formula of Helmholtz decomposition for horizontal wind (Equation 1) and the relation between horizontal wind u and v, with ψ and χ (Equation 2 and 3).

$$\vec{\mathcal{V}} = \vec{k}\,x\,\nabla\psi - \nabla\chi \tag{1}$$

$$u = -\frac{\partial\psi}{\partial y} - \frac{\partial\chi}{\partial x} \tag{2}$$

$$v = \frac{\partial\psi}{\partial x} - \frac{\partial\chi}{\partial y} \tag{3}$$

Singular Value Decomposition (SVD)

Singular value decomposition (SVD) was a mathematical tool used in climatology to establish a linear relationship between two datasets, such as Global Climate Model (GCM) and meteorological station rainfall data. In this study, 14 ensemble members of predictors were selected for monthly temporal resolution in seven windows. The SVD method produced two orthogonal spatial sets of a single vector, similar to an eigenvector or Empirical Orthogonal Function (EOF), but one for each variable. Additionally, it produces a single set of values associated with each vector pair, which was analogous to eigenvalues. For instance, two matrices, X and Y, with dimensions of t x p and t x q, were used for this purpose. Björnsson and Venegas (1997) provide more details on this topic (Equation 4).

$$X = \begin{pmatrix} x_{11} & \cdots & x_{1p} \\ | & \ddots & | \\ x_{t1} & \cdots & x_{tp} \end{pmatrix}$$
$$Y = \begin{pmatrix} Y_{11} & \cdots & Y_{1q} \\ | & \ddots & | \\ Y_{t1} & \cdots & Y_{tq} \end{pmatrix} \tag{4}$$

$X_{t\,x\,p}$ were the predictor values at t time in p grids, while $Y_{t\,x\,q}$ were the values of rainfall at t time in the q stations. The covariance matrix (Cxy) was (Björnsson and Venegas, 1997) in Equation (5).

$$C_{xy} = Z^T S \tag{5}$$

X and Y were centralized into Z and S, Z^T was the transpose matrix of the Z matrix (Equation 6).

$$Z = \begin{pmatrix} x_{11} & \cdots & x_{1p} \\ | & \ddots & | \\ x_{t1} & \cdots & x_{tp} \end{pmatrix} - \begin{pmatrix} \bar{x}_1 & \cdots & \bar{x}_p \\ | & \ddots & | \\ \bar{x}_i & \cdots & \bar{x}_p \end{pmatrix}$$
$$S = \begin{pmatrix} Y_{11} & \cdots & Y_{1q} \\ | & \ddots & | \\ Y_{t1} & \cdots & Y_{tq} \end{pmatrix} - \begin{pmatrix} \bar{Y}_1 & \cdots & \bar{Y}_q \\ | & \ddots & | \\ \bar{Y}_i & \cdots & \bar{Y}_q \end{pmatrix} \tag{6}$$

with $\bar{x}$ and $\bar{y}$ were the average of the i-th column of the X and Y matrix for i=1, 2, 3,..., p and for i=1, 2, 3,..., q.

$$A = L_1x_1 + L_2x_2 + \cdots\cdots + L_px_p = xL$$
$$B = N_1y_1 + N_2y_2 + \cdots\cdots + N_qy_q = yN \tag{7}$$

SVD find a linear combination of p predictor variables that having maximum covariance value with linear combination of q predicted variables. Linear combination pairs of A and B were called the expansion coefficients which analogous to an eigenvector or EOF (Equation 7).

$$C_{xy} = LDN^T \tag{8}$$

Correlation (r) on the most dominant mode expansion coefficient was between A and B, ranges from 0 (weak) to 1 (strong). Cross-covariance matrix in SVD decomposed into two orthogonal spatial pattern clusters and pairs with singular values (analogous to the eigenvalues). Decomposition of Matrix C_{xy} (Björnsson and Venegas, 1997) were in Equation (8). with L was singular matrix with dimension of p x m and N was singular matrix m x q dimension (m = min(p,q)).

$$SCF = \frac{\lambda_i^2}{\sum_{i=1}^{m}\lambda_i^2} \tag{9}$$

Matrix D was a non-negative diagonal matrix whose elements were $\lambda^1 > \lambda^2 > \ldots > \lambda^m$. Matrixes L and N sequentially can be determined by finding the singular vectors of $C_{xy}\,C_{xy}^T$ and $C_{xy}^T C_{xy}$ i.e. singular vectors $L_1, L_2, L_3, \ldots\ldots L_p$ and $N_1, N_2, N_3, \ldots\ldots N_p$ which correspond to the $\lambda_1^2 > \lambda_2^2 > \ldots > \lambda_m^2$. The corresponding of singular vectors L and N was described by a Square covariance fraction (SCF) (Equation 9).

RESULTS AND DISCUSSION

Expansion Coefficients Value

Monthly correlations between expansion coefficients A and B in the study area and the SCF were pre-

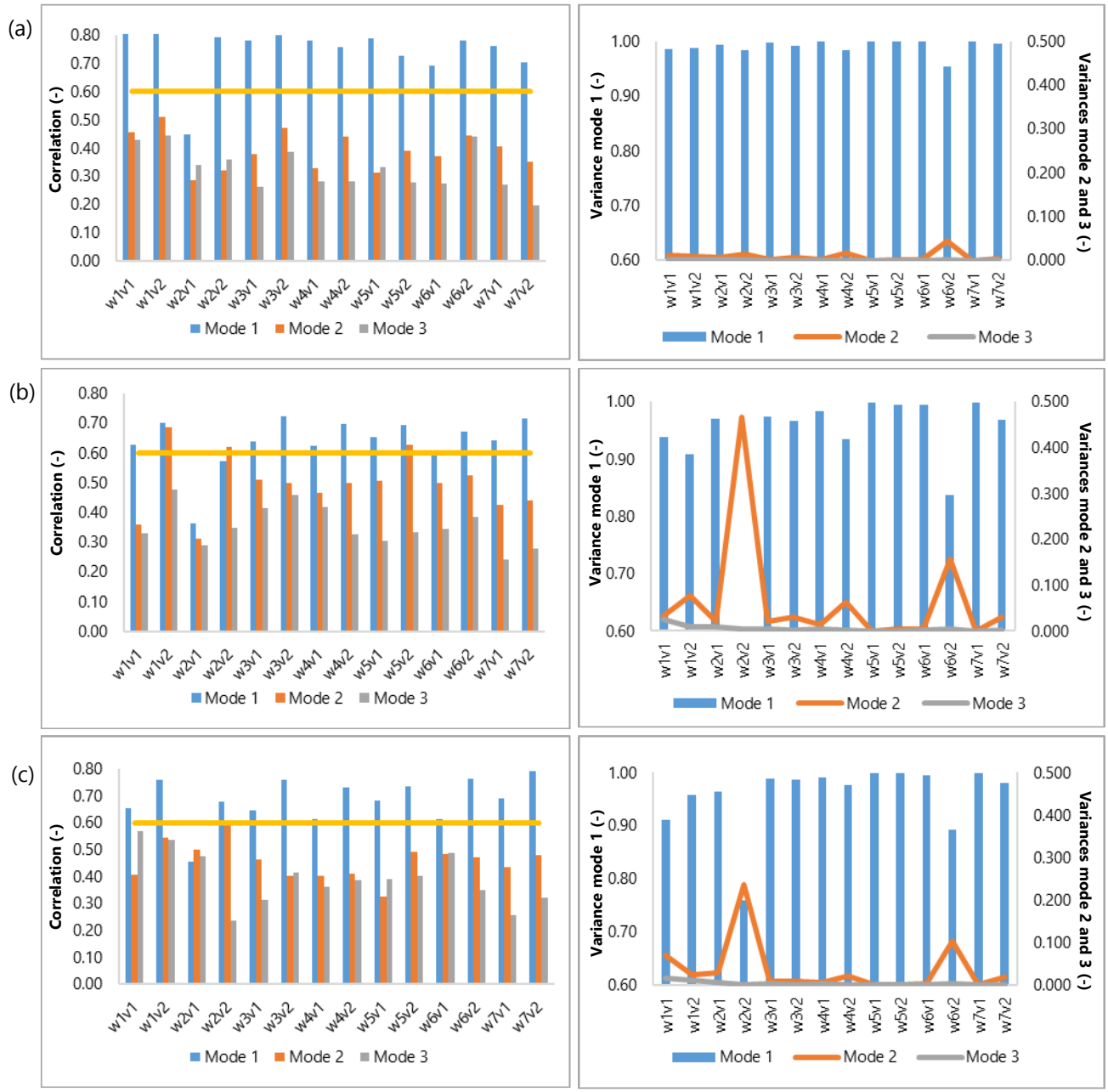

Figure 3. Correlation expansion coefficient A and B (two orthogonal spatial sets) (left panel) and Square Covariance Fraction (SCF) (right panel) for: (a) Java, (b) Sumatra, and (c) Borneo in Singular Value Decomposition (SVD) mode.

sented in Figure 3. The x-axis on graphs in Figure 3 were predictors in seven windows (w1 until w7) as seen in Figure 1, with parameters Phi (v1) and Psi (v2). In this study, the first mode had correlation values ranging from 0.45 to 0.83 in Java, 0.36 to 0.72 in Sumatra, and 0.45 to 0.79 in Borneo. The second mode had correlation values ranging from 0.29 to 0.51 in Java, 0.31 to 0.69 in Sumatra, and 0.32 to 0.59 in Borneo. The third mode had correlation values ranging from 0.20 to 0.57, with the highest value in Java and the lowest value in Sumatra. The correlation value between A and B indicated the relationship strength of the coupling pattern between rainfall and predictors (Psi and Phi).

Based on the SCF analysis, the three leading modes explain almost all the total square covariance between the predictors and rainfall in the study area (Figure 3). The first mode of all predictors had more than 0.95, except for predictors w2v2 and w6v2 in Sumatra and Borneo. The second mode SCF of predictors in Java was lower than 0.04 (see the second axis of the graphs), while in Sumatra, the highest was predictor w2v2 (0.47), followed by w6v2 (0.16). In addition, predictor w2v2 was the highest value for the second SCF of 0.24 in Borneo. The third mode SCF values were generally very low, less than 0.03, indicated a weak relationship between the predictors

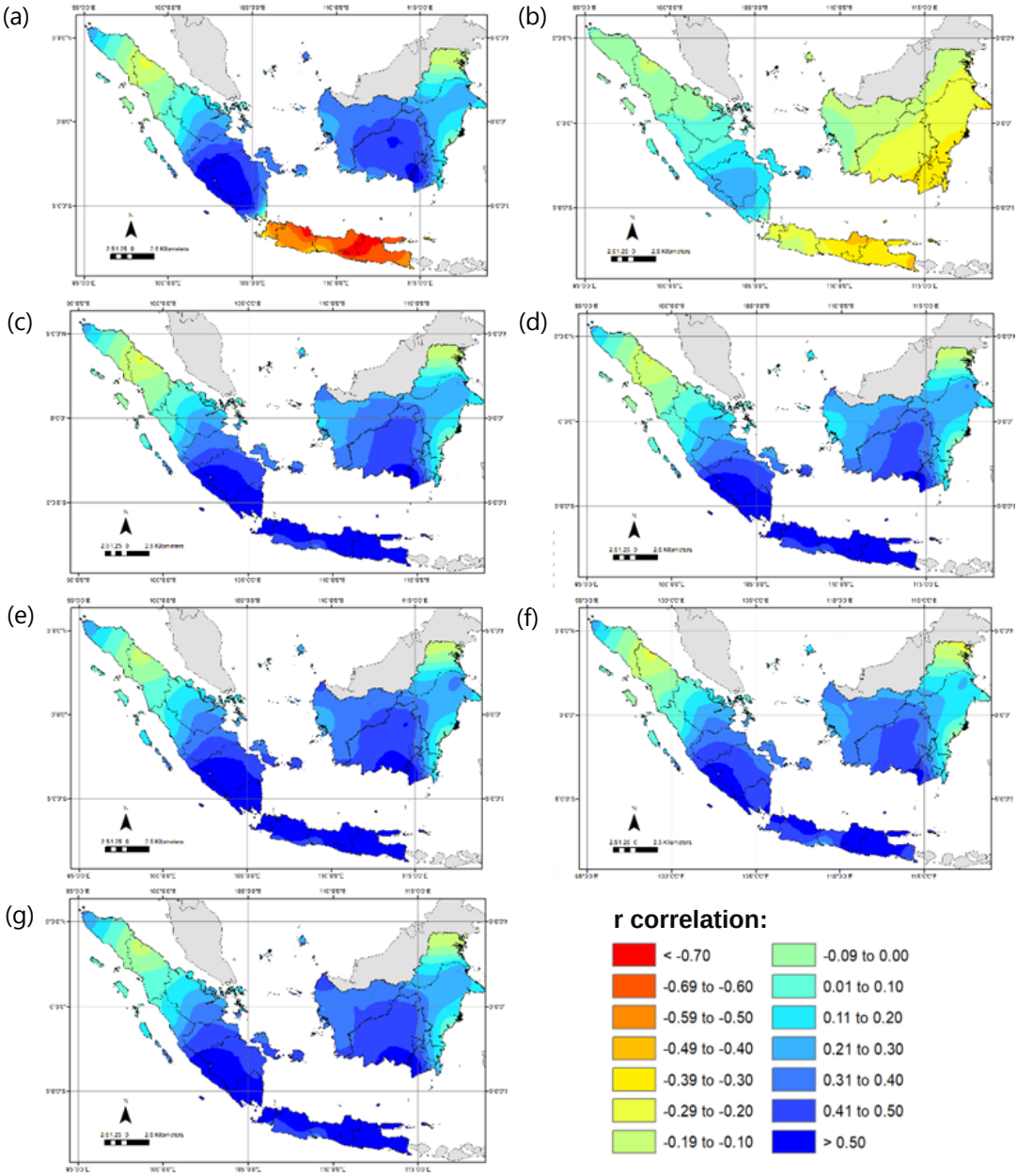

Figure 4. Correlation maps between expansion coefficients A mode 1 of predictor Phi in: (a) window 1, (b) window 2, (c) window 3, (d) window 4, (e) window 5, (f) window 6, and (g) window 7.

and rainfall for this mode. Overall, the SCF analysis suggested that the first and second modes of the predictors were the most important for explaining the variability in rainfall in the study area. The correlation maps indicated how well the information of expansion coefficients of predictors Phi and Psi can predict rainfall values. The correlation maps between expansion coefficients A mode 1 of predictor Phi with the values of rainfall at stations (y) or heterogeneous correlation map (Björnsson and Venegas, 1997) were presented in Figure 4.

The maps showed higher positive correlations in Java, the Southern part of Sumatra and Borneo for window 3 to window 7. On the contrary, the correlation in Java for window 1 had a higher correlation but in negative values, while in the Southern part of Sumatra and Borneo was positive. Window 1 or MCM, had a significant geographic seasonal variation due to the different sizes of islands interspersed around the surrounding sea (Chang et al., 2004), resulting in a different correlation in each island. The correlation was lower for windows 2 than other windows.

Correlation maps between expansion coefficients A of predictor Psi mode 1 with rainfall at stations were presented in Figure 5. The negative correlations between expansion coefficients A of predictor Psi mode 1 and rainfall values suggested that the amount of rainfall decreases as the value of A increases. This could imply a strong negative relationship between the flow patterns of Psi and rainfall in the study area.

The exception in window 2, where there was a positive correlation, could suggested a different rela-

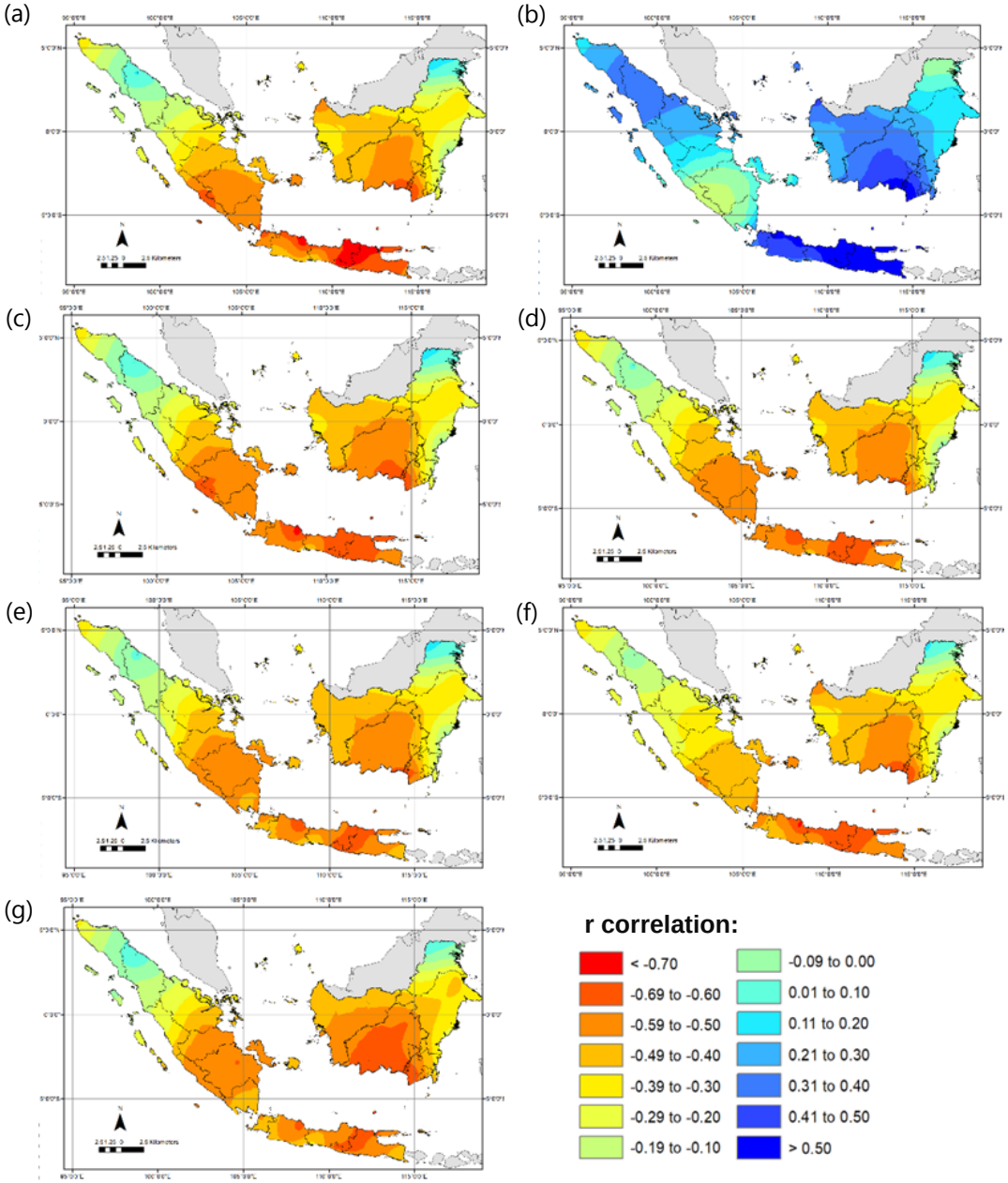

Figure 5. Correlation maps between expansion coefficients A mode 1 of predictor Psi in: (a) window 1, (b) window 2, (c) window 3, (d) window 4, (e) window 5, (f) window 6, and (g) window 7.

tionship between Psi and rainfall in that particular period or location. The finding by Kajikawa et al., (2010) of a significant anti-correlation between AUSMI anomalies and Asian monsoon onset date was interesting and suggests a potential link between the flow patterns in the study area and the monsoon onset.

Figures 6a and 6b presented correlation maps depicted the relationship between expansion coefficient B of rainfall mode one and predictors (Phi and Psi) across windows 1 to 7. The map in Figure 6a revealed negative correlations in northern latitudes, including the northern section of window 1 and windows 3 to 7, for predictor Phi. However, a positive correlation occured in southern latitudes, particularly in the southern part of window 1, except for window 2, which displays an exception with negative values. In contrast, the correlation map in Figure 6b between expansion coefficients B of rainfall mode 1 and predictor Psi illustrated a positive correlations in equatorial regions (0° to 10° N and S).

In addition, the correlations become negative as it moved away from the equator, including in windows 5, 7, and 3. It was noteworthy that window 2 exhibited a different spatial pattern than window 1. Figure 3 indicated that predictor w1v2 correlated with spatial rainfall patterns in Java, while w7v2 and w3v2 had the highest correlation in Sumatra. The predictor w7v2 also had the highest correlation in Borneo. On the other hand, predictor w2v1 had the lowest correlation

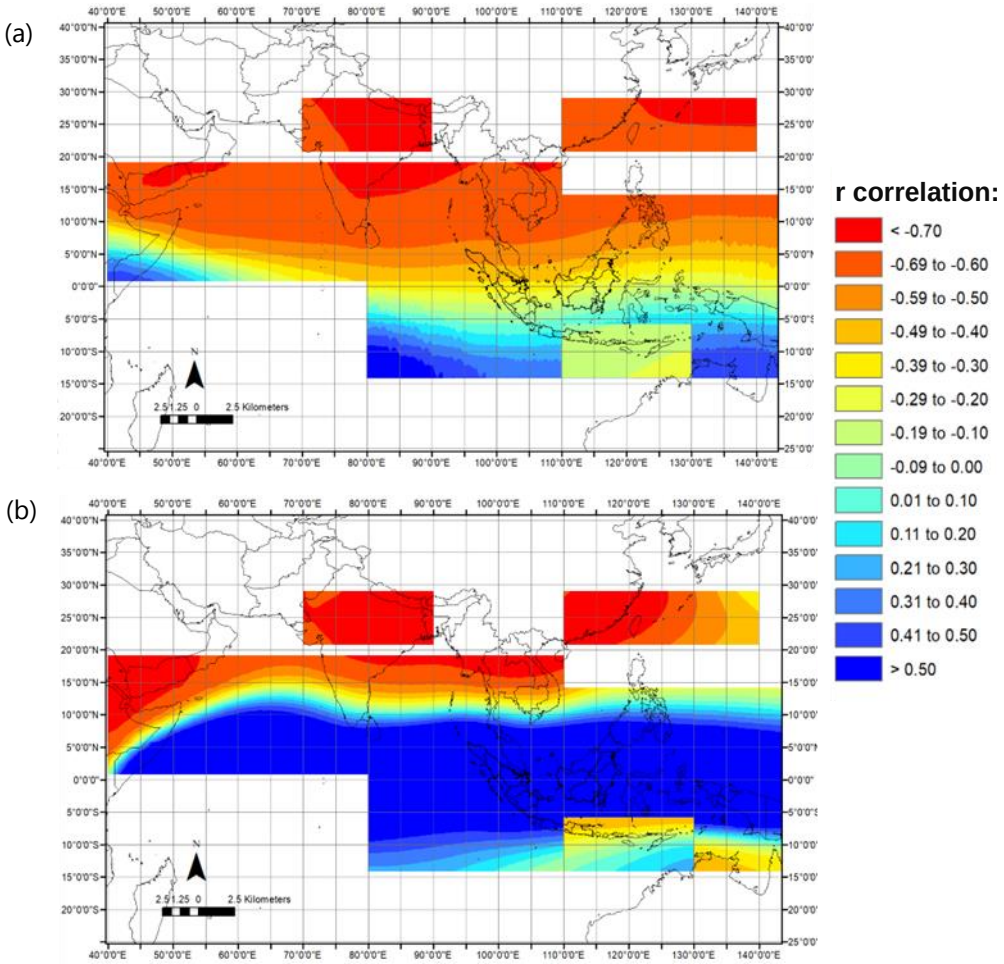

Figure 6. Correlation maps between expansion coefficients B mode 1 of rainfall with predictor Phi (a) and Psi (b) in windows 1 to 7.

value for all regions, indicating the weakest relationship with rainfall patterns in Java, Sumatra, and Borneo Islands.

Figure A1 presented the time series of expansion coefficients A and B in the first SVD mode for predictors which had the highest values of correlations in Java, Sumatra, and Borneo. Time series were smoothed 13 month running mean, and amplitudes of A and B were normalized by the relevant standard deviation (Björnsson and Venegas, 1997). Figure A1 can analyzed the dominant pattern of rainfall and predictor Psi. Both time series of A and B fluctuated inter-annually for all regions. The pattern of both parameters was similar but opposite.

According to the correlation maps presented in Figures 4 and 5, the predictor Psi showed higher correlations than Phi in Java, Sumatra, and Borneo. This was consistent with a previous Syahputra (2012) study, which found that Psi 850 mb was a better predictor than zonal wind u and Phi at the same altitude when using the single best analogue method. The correlation maps also revealed that the highest correlations occur in regions with a monsoonal rainfall type (Aldrian and Susanto, 2003), such as Java, the southern part of Sumatra, and Borneo, with predictors from the Asian monsoon (windows 1, and 3 up to 7). However, window 2, or the AUSMI window, exhibits a different pattern. This may be due to the dominant influence of the Australian monsoon over Asia, resulting in an anti-correlation with rainy season onset (Kajikawa et al., 2010). Interestingly, the correlation of predictor Psi in window 2 was higher than that of Phi.

The second mode of SCFs in Sumatra and Borneo was higher than in Java, specifically in windows 2 and 6 of predictor Phi, indicating that the rainfall variability in Sumatra and Borneo was higher than in Java (Figure 3). This was consistent with the semi-monsoonal rainfall types observed in the Northern part of Sumatra and the Western and Northern parts of Borneo, which had two peak annual rainfall patterns. In contrast, Java had a monsoonal type (Salmayenti et al., 2017; Qian et al., 2010). In a similar study, Safril and Virgianto (2018) also utilized SVD analysis to select rainfall predictors for Sumatra Island in the maritime continent domain based on the rainfall types observed in Sumatra. They found that zonal wind 850 mb was closely related to Sumatra's monsoon and semi-monsoonal rainfall.

CONCLUSIONS

This study investigates ERA-20C wind field Predictors (Phi and Psi) in seven monsoon window domains to select the best potential predictor from seven monsoon windows. The selection was based on spatial pattern correlation A and B because the SCF for all windows mostly was high. The predictor Psi in MCM (80°–150° E and 15° S–15° N) window was the highest for Java, while Sumatra and Borneo were predictor Psi of WNPSM (110°–140° E and 20°–30° N). The lowest correlation for all regions was predictor Phi in AUSMI (110°–130° E and 5°–15° S) window. SVD analysis in this study was a pre-processing step for ensemble rainfall prediction using the multi-windows approach to quantify the uncertainty. The result of SVD can be used to eliminate predictors that had weaker relation to the rainfall prediction and to reduce the error from GCM predictors.

ACKNOWLEDGEMENT

The authors thank Indonesia Endowment Fund for Education (LPDP) for funding the research and acknowledge Indonesia Agency for Meteorology Climatology and Geophysics (BMKG) for facilitating the rainfall data. TW drafted the initial manuscript, and all the authors were involved in discussions during the manuscript process. This Paper is part of a Dissertation with additional of analysis and study area.

REFERENCES

Aldrian, E., Susanto, R.D., 2003. Identification of three dominant rainfall regions within Indonesia and their relationship to sea surface temperature. International Journal of Climatology: A Journal of the Royal Meteorological Society 23, 1435–1452.

Beck, C., Philipp, A., Streicher, F., 2013. The effect of domain size on the relationship between circulation type classifications and surface climate. International Journal of Climatology 36, n/a-n/a. https://doi.org/10.1002/joc.3688.

Björnsson, H., Venegas, S.A., 1997. A manual for EOF and SVD analyses of climatic data (No. CCGCR Report 97).

Caillouet, L., Vidal, J., Sauquet, E., Graff, B., Soubeyroux, J., 2019. SCOPE Climate: a 142-year daily high-resolution ensemble meteorological reconstruction dataset over France. Earth System Science Data 11, 241–260.

Cao, J., Xu, Q., Chen, H., Ma, S., 2022. Hybrid Methods for Computing the Streamfunction and Velocity Potential for Complex Flow Fields over Mesoscale Domains. Advances in Atmospheric Sciences 39, 1417–1431. https://doi.org/10.-1007/s00376-021-1280-y.

Donat, M. G., Alexander, L. V., Yang, H., Durre, I., Vose, R., & Caesar, J. 2013. Assessment of a statistical downscaling technique for projecting local-scale meteorological data from global reanalysis products. International Journal of Climatology 33, 2473-2491. doi: 10.1002/joc.3609.

Dutton, J.A., 1976. Solutions to Problems in The Ceaseless Wind: An Introduction to the Theory of Atmospheric Motion. Pennsylvania State University.

Hammond, M., Lewis, N.T., 2021. The rotational and divergent components of atmospheric circulation on tidally locked planets, in: Proceedings of the National Academy of Sciences 118. p. e2022705118.

Hashiguchi, H., Shoji, Y., Tsuda, T., Shibagaki, Y., Kumagai, H., Yamanaka, M. D., & Syamsudin, F. 2011. Classification of Indonesian rainfall based on characteristic patterns of diurnal variation. Journal of the Meteorological Society of Japan, 89A, 117-139. doi: 10.2151/jmsj.2011-A05.

Hendon, H.H., 2003. Indonesian rainfall variability: Impacts of ENSO and local air–sea interaction. Journal of Climate 16, 1775–1790.

Hendrawan, I.G., Asai, K., Triwahyuni, A., Lestari, D.V., 2019. The interanual rainfall variability in Indonesia corresponding to El Niño Southern Oscillation and Indian Ocean Dipole. Acta Oceanologica Sinica 38, 57–66. https://doi.org-/10.1007/s13131-019-1457-1.

Hersbach, H., Peubey, C., Simmons, A., Berrisford, P., Poli, P., Dee, D., 2015. ERA - 20CM: A twentieth - century atmospheric model ensemble. Quarterly Journal of the Royal Meteorological Society 141, 2350 – 2375.

Jin, H., Jiang, W., Chen, M., Li, M., Bakar, K.S., Shao, Q., 2023. Downscaling long lead time daily rainfall ensemble forecasts through deep learning. Stochastic Environmental Research and Risk Assessment. https://doi.org/10.1007/s00477-023-02444-x.

Kajikawa, Y., Wang, B., Yang, J., 2010. A multi - time scale Australian monsoon index. International Journal of Climatology 30, 1114 – 1120.

Lee, H.S., 2015. General Rainfall Patterns in Indonesia and the Potential Impacts of Local Seas on Rainfall Intensity. Water 7, 1751–1768. https://doi.org/10.3390/w7041751.

Li, Z., Chao, Y., McWilliams, J.C., 2006. Computation of the streamfunction and velocity potential for

limited and irregular domains. Monthly weather review 134, 3384–3394.

Mason, S.J., Baddour, O., 2008. Statistical modelling. In Seasonal climate: forecasting and managing risk. Springer, Dordrecht.

Moron, V., Robertson, A.W., Qian, J., 2010. Local versus regional-scale characteristics of monsoon onset and post-onset rainfall over Indonesia. Climate dynamics 34, 281–299.

Palmer, C.E., 1952. Reviews of modern meteorology—5. Tropical meteorology. Quarterly Journal of the Royal Meteorological Society 78, 126–164.

Poli, P., Hersbach, H., Dee, D.P., Berrisford, P., Simmons, A.J., Vitart, F., Laloyaux, P., Tan, D.G., Peubey, C., Thépaut, J.N., Trémolet, Y., 2016. An atmospheric reanalysis of the twentieth century. Journal of Climate 29, 4083–4097.

Qian, J., Robertson, A., Moron, V., 2010. Interactions among ENSO, the Monsoon, and Diurnal Cycle in Rainfall Variability over Java, Indonesia. Journal of The Atmospheric Sciences - J ATMOS SCI 67, 3509–3524. https://doi.org-/10.1175/2010JAS3348.1.

Hidayat, R., Ando, K., 2014. Rainfall Variability over Indonesia and its relation to ENSO/IOD: Estimated using JRA-25/JCDAS. Agromet 28, 1-8.

Ramage, C.S., 1968. Role of a tropical "maritime continent" in the atmospheric circulation. Monthly Weather Review 96, 365–370.

Robertson, A.W., Moron, V., Qian, J., Chang, C., Tangang, F., Aldrian, E., Koh, T.Y., Liew, J., 2011. The maritime continent monsoon.

Safril, A., Virgianto, R.H., 2018. Studi Potensi Variabel Angin Zonal sebagai Prediktor untuk Wilayah Benua Maritim (Studi Kasus Sumatera). Jurnal Meteorologi Klimatologi dan Geofisika 5, 26–39.

SPARC, 2022. Reanalysis Intercomparison Project (S-RIP) Final Report (Project No. SPARC Report No.10, WCRP-6/2021).

Salmayenti, R., Hidayat, R., Pramudia, A., 2017. Rainfall Prediction Using Artificial Neural Network. Agromet 31, 11-21. https://doi.org/10.29244/-j.agromet.31.1.11-21

Surmaini, E., Hadi, T.W., Subagyono, K., Puspito, N.T., 2015. Prediction of drought impact on rice paddies in west Java using analogue downscaling method. Indonesian Journal of Agricultural Science 203.

Syahputra, M., 2012. Kajian Prakiraan Curah Hujan Musiman Dengan Metode CA (*Constructed Analogue*) dari Keluaran Model CFS (*Climate Forecast System*) Studi Kasus: Pulau Jawa Dan Sumatera). JTM 19.

Wang, B., Wu, R., Lau, K.M., 2001. Interannual variability of the Asian summer monsoon: Contrasts between the Indian and the western North Pacific–East Asian monsoons. Journal of climate 14, 4073–4090.

Wati, T., Wigena, A.H., 2014. Seleksi prediktor data global climate model dengan teknik singular value decompotition untuk prediksi curah hujan di pantai utara jawa barat. Junal Meteorologi dan Geofisika 15.

Webster, P.J., Yang, S., 1992. Monsoon and ENSO: Selectively interactive systems. Quarterly Journal of the Royal Meteorological Society 118, 877–926.

Wilby, R.L., Charles, S.P., Zorita, E., Timbal, B., Whetton, P., Mearns, L.O., 2004. Guidelines for use of climate scenarios developed from statistical downscaling methods.

ANNEX

Figure A1. Time series of expansion coefficient A and B (two orthogonal spatial sets) mode 1 of predictor (a) window 1-Psi in: Java, (b) window 7-Psi in Sumatra, (c) Borneo.

(a)

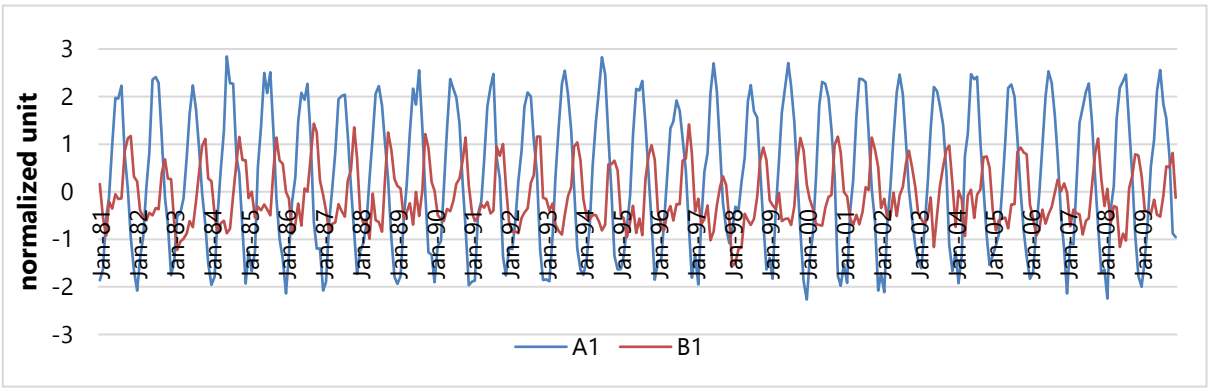

(b)

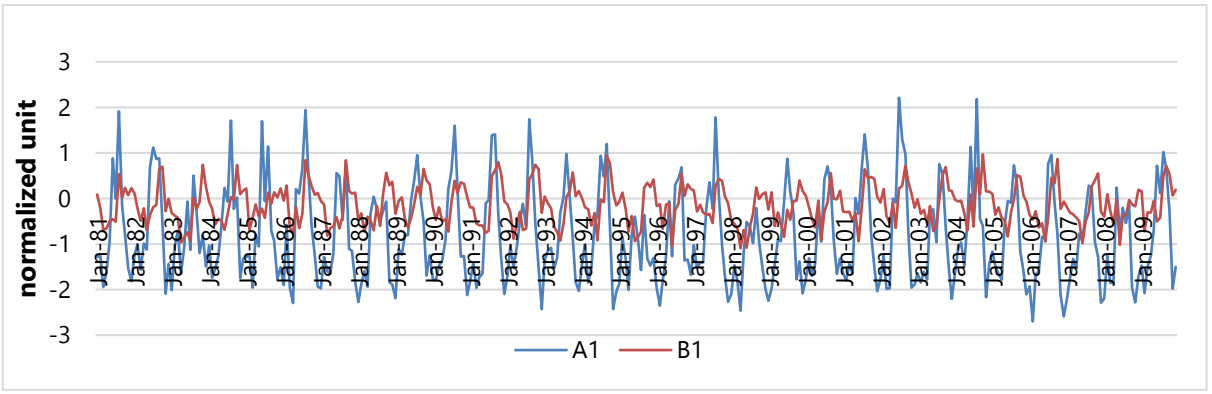

(c)